

Production of bacterial nanocellulose from wine industry residues: Importance of fermentation time on pellicle characteristics

Patricia Cerrutti,^{1,2} Pamela Roldán,¹ Ricardo Martínez García,^{3,4} Miguel A. Galvagno,^{2,3,5}
Analia Vázquez,^{1,3} María L. Foresti^{1,3}

¹Biotechnology and Biosynthesis Group, Institute of Technology in Polymers and Nanotechnology (ITPN), Engineering Faculty, University of Buenos Aires, Argentina

²Chemical Engineering Department, Engineering Faculty, University of Buenos Aires

³National Scientific and Technical Research Council (CONICET), Argentina

⁴Natural Resources Faculty, National University of Formosa, University Campus, Formosa, Argentina

⁵IIB-INTECH-UNSAM (Institute of Biotechnological Research), San Martín Buenos Aires, Argentina

Correspondence to: M. L. Foresti (E-mail: mforesti@fi.uba.ar)

ABSTRACT: Bacterial nanocellulose (BNC) was produced by *Gluconacetobacter xylinus* under static conditions using grape pomace extract (the most abundant residue of the wine industry) as a carbon source and corn steep liquor (a byproduct of corn wet-milling) as the main nitrogen source. Carbon and nitrogen source concentrations, as well as inocula size, fermentation time, and temperature, were all considered in order to maximize BNC production by the use of statistically designed experiments and the response surface methodology. At optimum production conditions, the effect of fermentation time on morphology, solids content, chemical structure, crystallinity, thermal decomposition pattern, and storage modulus of dried BNC pellicles was analyzed. The results evidenced that dried BNC pellicles that were incubated for longer times showed higher thermal stability, higher crystallinity, and higher storage modulus, resulting from a denser nanoribbons network. All of these characteristics will certainly play a role in the performance of BNC in practical applications. © 2015 Wiley Periodicals, Inc. *J. Appl. Polym. Sci.* **2016**, *133*, 43109.

KEYWORDS: biopolymers and renewable polymers; biosynthesis of polymers; cellulose and other wood products

Received 11 August 2015; accepted 29 October 2015

DOI: 10.1002/app.43109

INTRODUCTION

Cellulose is a polymer composed of glucose units connected by β (1–4) glycosidic linkages. It is very abundant in nature because it is the main component of the cell wall of plants. However, due to the simultaneous presence of lignin and hemicelluloses, fine chemical applications of vegetable cellulose usually require the implementation of different treatments (mechanical, chemical, and/or enzymatic) aimed at isolating a pure compound. However, mechanical methods (e.g., grinding, refining, cryocrushing, high-intensity ultrasonication) are energy-consuming, usually demanding high levels of pressure or kinetic energy. On the other hand, chemical pulping aimed at dissolving hemicellulose and lignin (e.g., Kraft process, organic solvent extraction, acidic methods, liquid phase oxidation) normally induce a great deal of simultaneous carbohydrate degradation, and the environmental impact of the byproducts and residues of the process needs to be considered. Finally, enzymatic pulping methods, in which

enzymes (e.g., xylanases, pectinases, and ligninases) directly depolymerize specific components of the matrix in which cellulose is embedded, induce much lower cellulose degradation, but the high price of the hydrolytic enzymes required is often prohibitive for commercial purposes.

On the other hand, identical cellulose in terms of molecular structure can be obtained from several microorganisms, such as algae, molds, and bacteria of the genera *Acetobacter*, *Agrobacterium*, *Alcaligenes*, *Pseudomonas*, *Rhizobium*, *Aerobacter*, *Achromobacter*, *Azotobacter*, *Salmonella*, and *Sarcina*. Among bacteria, *Gluconacetobacter xylinus* (formerly *Acetobacter xylinum*) has been reported as capable of producing bacterial nanocellulose (BNC) in commercial quantities.¹ *G. xylinus* secretes cellulose at the air–liquid interface as a fine and well-ordered structure, built up by nanofibers of rectangular cross section with thicknesses around 3–10 nm, 30–100 nm in width, and 1–9 μm in length.^{2–4} The polymer thus obtained is a nanostructured, highly pure extracellular compound with unique

Additional Supporting Information may be found in the online version of this article

© 2015 Wiley Periodicals, Inc.

physicochemical, biological, and mechanical properties, such as high water-holding capacity, high crystallinity, low thermal expansion coefficient in the axial direction, high tensile strength and Young's modulus, and biodegradability and biological adaptation.

Gluconacetobacter xylinus can use a variety of substrates as carbon source for BNC production, such as glucose, fructose, sucrose, xylose, arabinose, mannitol, arabitol, glycerol, and oligosaccharides.^{1,5–7} Nowadays, when the goal is the production of BNC at a large scale, lower costs are required to obtain an economically feasible process. Because the current price of the Hestrin and Schramm medium (the one typically used for BNC production) limits most industrial uses, in the last few years a number of agroindustrial byproducts or residues have been proposed as nonconventional cheaper sources of C or N for high-value BNC production.^{7–15}

For each strain used, BNC production depends on the selected C or N source and on the C/N ratio used, and there is no general pattern of bacterial behavior in a given species that can lead to the selection of the most appropriate conditions.¹⁶ So, for the first approach, statistical screening designs can be used to establish the variables that significantly influence BNC production and to estimate their magnitude. Then, the optimization of the selected parameters can be performed by changing one factor at a time or by employing statistical methods that aim to optimize a process given a reduced number of variables.

In the current contribution, statistical design of experiments (DoEs) and a response surface methodology (RSM) analysis were used to maximize the production of BNC when *G. xylinus* and a nonconventional inexpensive C source such as grape pomace extract (GE) were employed. Wine production is one of the most important agricultural activities throughout the world. The wine industry consumes a considerable amount of resources such as water, fertilizers, and organic amendments and produces a large amount of wastewater and organic wastes characterized by high contents of biodegradable compounds and suspended solids.¹⁷ Among them, grape pomace is the most abundant residue left after juice extraction and does not require difficult or expensive pretreatments, as lignocellulosic feedstocks do. Grapes provide the fermentable sugars D-glucose and D-fructose that can be used as renewable C and energy sources as well as cellulose precursor. Corn steep liquor (CSL), a byproduct of corn wet-milling, was used as the main N source.

Under optimum BNC production conditions, the next aim of the current contribution was to evaluate how fermentation time affects the morphology, solids content, chemical structure, thermal decomposition properties, crystallinity, and definite mechanical properties of dried BNC pellicles, which will certainly condition their behavior in practical applications. In static cultures, BNC production is generally carried out over 7 to 14 days.^{7,9,13–15} However, depending on the desired application, shorter or longer times may lead to BNC membranes with more appropriate properties.

MATERIALS AND METHODS

Microorganism and Reagents

The bacterial strain of *G. xylinus* (syn. *Acetobacter aceti* subsp. *xylinus*, *Acetobacter xylinum*) NRRL B-42 used in this work was graciously provided by Dr. Luis Ielpi (Fundación Instituto

Leloir, Buenos Aires, Argentina), and it was maintained at -80°C in glycerol 20% (v/v).

The seeds and stems of pomace from Semillon grapes pressed for wine-making were separated, and the remaining raw material (skins and residual pulp) were washed three times with distilled water and then homogenized in a Waring blender using a minimum required volume of 0.10 M citric acid–sodium citrate buffer at pH = 5.0. The grape extract obtained was filtered through cheesecloth and centrifuged ($5000 \times g$ for 5 min at 4°C) to separate solids, and the clarified liquid filtrate was frozen at -20°C until used. The reducing sugar (RS) content in GE (D-glucose plus D-fructose), was determined by dinitrosalicylic acid assays with D-glucose as a standard solution. The RS content was confirmed with an enzymatic kit that detects D-glucose and D-fructose (Boehringer Mannheim/R-Biopharm (Mannheim, Germany), catalog no. 10716260035). Finally, GE was diluted in order to reach the RS values stated by the matrix of each design or required for each experiment.

Corn steep liquor was graciously provided by Ingredion Argentina S.A. (Baradero, Argentina) with the following nitrogen fraction composition (% protein): protein (nonhydrolyzed), 15.0; peptides, 35.0; free amino acids, 35.0; amines, 2.0; NH_4^+ , 1.0; NH_3 , 10.0; purine, pyrimidine, and derivatives, 2.0. The CSL also provided (% w/w; dry basis) 0.06 calcium and 15–20 lactic acid.

Culture Conditions

Inocula were cultured at 28°C for 48 h in 100 mL Erlenmeyer flasks containing 20 mL of Hestrin and Schramm (HS) medium (% w/v): anhydrous dextrose (Biopack, Zarate, Argentina), 2.0; meat peptone (Britania, Laboratorios Britania S.A.), 0.5; yeast extract (Britania, Laboratorios Britania S.A., CABA, Argentina), 0.5; anhydrous disodium phosphate (Anedra, San Fernando, Argentina), 0.27; citric acid (Merck, Carlos Spegazzini, Argentina), 0.15. The pH was adjusted to 6.0 with dilute HCl or NaOH. Culture agitation (200 rpm) was provided by an orbital shaker. Direct microscope counts were performed to estimate the bacterial inoculum concentration.

For BNC production, aliquots of 1 mL of the inoculum (3×10^8 cells mL^{-1}) were transferred to 250 mL Erlenmeyer flasks containing 100 mL of aqueous media with GE and CSL at the concentrations stated by the matrices of the designs, unless indicated. After the established incubation times in static conditions at the selected temperatures, BNC pellicles were harvested and rinsed with water to remove the culture medium.

To calculate BNC production (g L^{-1}) and productivity ($\text{g L}^{-1} \text{days}^{-1}$), the pellicles were boiled in 2% w/v NaOH solution for 1 h in order to eliminate the bacterial cells from the cellulose matrix, washed with distilled water to neutralization, and dried in a thermobalance Precisa XM50 (Dietikon, Switzerland) at 105°C to constant weight.

Experimental Designs

Fractional factorial screening designs were applied to determine the culture variables that may significantly affect cellulose production. These designs were set up for five factors with three coded levels ($-1, 0, +1$). Three repetitions of the center point were run for each experiment. The results were fitted with a

first-order model, estimating the coefficient for each factor and its level of significance.^{18,19}

Box-Behnken designs (BBD)²⁰ set up for three factors at three coded levels (-1, 0, +1) were run to evaluate the linear and quadratic effects and two-way interactions among the variables and to construct a second-order polynomial model. The variable ranges were selected according to the results of the screening designs, and three repetitions of the center point were run in order to determine the experimental error. In all of the designs, the variable levels X_i were coded as x_i according to eq. 1:

$$x_i = \frac{X_i - X_0}{\Delta X_i}, \quad i=1, 2, 3, \dots, k \quad (1)$$

where x_i and X_i are the dimensionless codified value and the actual value of an independent variable, respectively, X_0 is the real value of an independent variable at the center point, and ΔX_i is the step change.

The RSM was used to analyze the experimental design. The second-degree model used to fit the response to the independent variables is shown in eq. 2:

$$Y = \beta_0 + \sum \beta_{ij} x_i x_j + \sum \beta_{ii} x_i^2 \quad (2)$$

where Y is the predicted response, x_i and x_j are the input variables that influence the response variable (Y), β_0 is the intercept, β_i is the i th lineal coefficient, β_{ii} is the i th quadratic coefficient, and β_{ij} is the ij th interaction coefficient.

Statistical and numerical analyses were carried out by analysis of variance (ANOVA) and multiple regression using the software Essential Regression (Experimental Design in MS Excel-free, user-friendly software package, v. 2003). The responses measured were subjected to multiple regression by least squares. The statistical significance of the coefficients obtained was evaluated by Student's t test. The adequacy of the mathematical models of the regression was assessed with Fisher's F test. All experimental designs were randomized to exclude bias and carried out at least in duplicate and repeated at least twice.

Characterization of BNC Pellicles: Analysis of Fermentation Time Effects

Scanning Electron Microscopy (SEM). Pieces of BNC pellicles (5 mm by 5 mm) were coated with gold using an ion sputter coater and observed by use of a scanning electron microscope Zeiss Supra 40 (Dresden, Germany) with a field emission gun operated at 3 kV.

Fourier Transform Infrared Spectroscopy (FTIR). Fourier transform infrared spectra of ground samples were acquired on an IR Affinity-1 Shimadzu Fourier transform infrared spectrophotometer (Kyoto, Japan) in transmission mode. Carefully dried (10 mg, 105 °C, 1 h) ground BNC samples were mixed with previously dried (130 °C, overnight) KBr in the ratio 1:25. The prepared pellets were further dried overnight at 105 °C, and spectra were collected with 40 scans in the range of 4000 to 700 cm^{-1} with a resolution of 4 cm^{-1} . The samples were normalized against the band found at 1165 cm^{-1} assigned to the (C—O—C) link of cellulose.^{21,22}

X-ray Diffraction (XRD). The diffraction patterns of ground BNC samples were obtained in a Rigaku D/Max-C wide-angle

automated X-ray diffractometer (San Pablo, Brazil) with vertical goniometer. The X-ray diffraction patterns were recorded in a 2θ angle range of 10 to 45 ° at a step size of 0.02 °. The wavelength of the Cu K α radiation source used was 0.154 nm, generated at accelerating voltage of 40 kV and a filament emission of 30 mA. In order to calculate the crystallinity (C) of the BNC samples, a deconvolution with the use of Lorentzian functions was performed. The average crystallite size (D) was estimated from the Scherrer equation, $D = 0.94\lambda / \beta \cos\theta$.²⁵ The Scherrer equation parameters are as follows: λ is the X-ray wavelength (Cu K α = 1.4518 Å), β is the line broadening, and θ is the Bragg angle. To subtract instrumental effects, a deconvolution of the XRD peaks was done using a silicon standard pattern.

Thermogravimetric Analysis (TGA). Thermogravimetric analyses of dried ground samples (2.5–3 mg, 105 °C, 1 h) were conducted in a TGA-50 Shimadzu instrument (Kyoto, Japan). Temperature programs were run from 25 °C to 800 °C at a heating rate of 10 °C/min under nitrogen atmosphere (30 mL/min) in order to prevent thermoxidative degradation.

Dynamic Mechanical Analysis (DMA). The dynamic mechanical responses of the dried BNC pellicles (10 mm × 5 mm × 0.05 mm) were measured using a dynamic mechanical analyzer Perkin Elmer DMA 8000 (Massachusetts, USA) in tension mode. The storage modulus (E') was computed as a function of temperature in the range of 30 to 100 °C under a constant heating rate of 2 °C/min, after preconditioning of samples at 30 °C for 10 min in the DMA chamber. The frequency of the sinusoidal strain imposed on the samples was 1 Hz. The displacement was fixed at 0.012 mm to guarantee measurement in the elastic response range. The measurements were performed in triplicate.

RESULTS AND DISCUSSION

BNC Production: Experimental Designs

A fractional factorial design was applied in order to screen out the effects of culture variables that could significantly affect BNC production. The variables proposed were the RS concentration coming from the GE content ($X_1 = 10.0$ – 60.0 g L^{-1}), CSL concentration ($X_2 = 0.0$ – 2.0 g L^{-1}), logarithm of the initial inoculum concentration ($X_3 = 4$ – 6), fermentation temperature ($X_4 = 24$ – 37 °C), and time of incubation ($X_5 = 4$ – 20 days). Table S1 (in the Supporting Information) shows the experimental and coded values of the variables studied, the response obtained, expressed as BNC production (g L^{-1}), and the equation obtained, where significant variables, i.e., GE content and incubation time, have been highlighted.

Based on the results obtained from the screening designs, and given the high importance of C/N ratio on the balance of cell growth/BNC production,¹ optimization experiments including the RS concentration in GE (10–70 g L^{-1}), CSL concentration (10–20 g L^{-1}), and incubation time (5–25 days) were conducted using BBD designs. Table S2 (Supporting Information) summarizes the experiments run and the corresponding BNC production obtained. In addition, Figure 1 shows a three-dimensional (3D) RSM plot of BNC production versus nutrient concentrations (25 days), illustrating the optimum region predicted for maximizing cellulose production. Further details on the

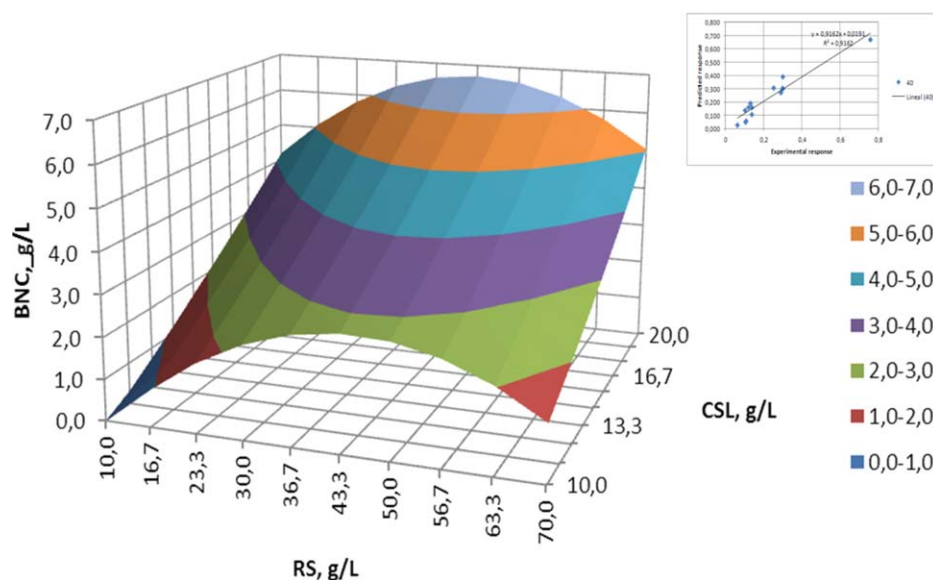


Figure 1. Response surface plot showing the effect of reducing sugars from grapes and corn steep liquor concentrations on bacterial nanocellulose production for Box-Behnken optimization design at 25 days of incubation at 28 °C. Inset: Predicted versus experimental responses for Box-Behnken optimization design. [Color figure can be viewed in the online issue, which is available at wileyonlinelibrary.com.]

mathematical equation obtained, the statistical analysis of results, factors effects, and ANOVA analysis have been included in the Supporting Information (Table S3).

The optimum BNC production value predicted by the model (6.7 g L^{-1}) and the validation assay result (6.56 g L^{-1} , triplicate), were much higher than the ones estimated in the previous designs assayed and corresponded to 43.1 g L^{-1} RS, 20.0 g L^{-1} CSL and 25 days of incubation. Compared with a traditional BNC biosynthesis medium, under identical conditions, BNC production in the Hestrin and Schramm medium was $\sim 1.4 \text{ g L}^{-1}$, a value 80% lower than the one achieved in the grape pomace/corn steep liquor medium herein proposed. Moreover, compared with the literature, BNC production values ranging from 3 to 11 g L^{-1} have been reported when different species of the *Gluconacetobacter* genus were grown in static systems using agroindustrial byproducts and residues such as pineapple peel juice,⁹ coffee cherry husk extract,^{8,13} distillery wastewater,⁷ pineapple solid waste,¹⁵ and agriculture residue hydrolysates.²³

Corn steep liquor, a raw material cheaper than peptones or yeast extract, may have contributed to enhance the production achieved in the grape pomace medium because it not only provided N (in the form of proteins, peptides, aminoacids, amines, NH_4/NH_3 , or N bases) but also organic acids, carbohydrates, vitamins, and minerals, and it is also reported to exert a buffering effect on the culture medium. In particular, it contains Ca^{2+} , which can activate cellulose synthase, thus increasing BNC production.^{24,25} Also, Wang *et al.*²⁶ reported that organic acids such as lactic acid (present in CSL) or acetic or pyruvic acids could enhance the cellulose yield. Moreover, Matsuoka *et al.*²⁷ used CSL in a fermentation medium formulation to produce BNC with a strain of *A. xylinum* subsp. *sacrofermentans* and reported that lactate could stimulate cell growth by linking with the respiratory chain and generating energy for growth. These authors speculated that lactate could act as an accelerator

driving the tricarboxylic acid cycle and as an energy producer, resulting in high cellulose production and rapid cell growth. They also reported that L-methionine, an amino acid present in CSL, could be essential for high cellulose yields and stimulation of cell growth during the early stage of the culture.

Fermentation Time Effects

In the optimized medium composition determined in the previous section, the effect of incubation time on BNC production, productivity, and chosen dried pellicle characteristics was evaluated. Figure 2 illustrates the evolution of BNC production and productivity as a function of incubation time. As is shown, production increases with fermentation time up to 21 days, whereas for longer incubation intervals BNC production increases only marginally. Note that the productivity data show two maxima at 5 ($0.38 \text{ g L}^{-1} \text{ day}^{-1}$) and 21 days ($0.31 \text{ g L}^{-1} \text{ day}^{-1}$) of fermentation.

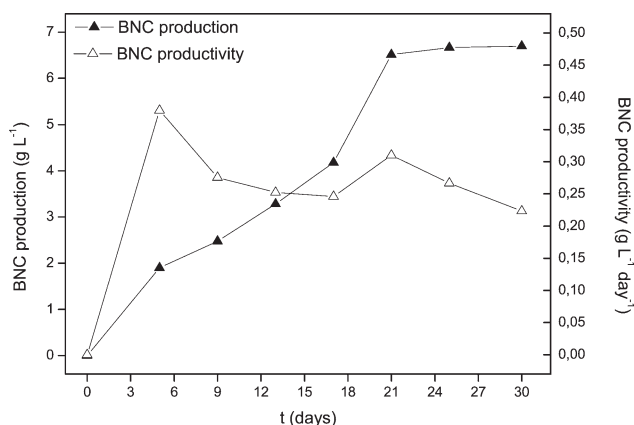


Figure 2. Evolution of production and productivity of BNC in the optimized medium at 28 °C.

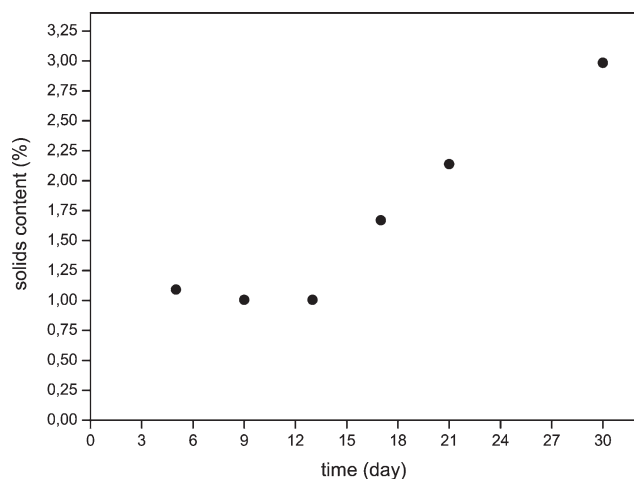


Figure 3. Solids content (%) of BNC pellicles obtained for increasing fermentation intervals.

BNC hydrogels incorporate large amounts of water, being the solids content of BNC pellicles obtained in static culture generally below 2–3%. The incorporated water plays an important role as a spacer element and as a stabilizing agent with respect to the network and pore structure.²⁸ BNC pellicles harvested from the fermentation medium for increasing incubation times were boiled in NaOH solution, properly washed with distilled

water to neutralization, and dried at 105 °C to constant weight. The weight ratio of dried pellicle to never-dried pellicle was calculated as a measure of the solid fraction of the BNC samples. The results have been included in Figure 3.

As shown, the BNC membranes obtained within the first 13 days of fermentation have solids contents in the 1.0–1.1% range, whereas the solids content of membranes obtained with longer incubation periods is significantly higher: 1.7–3.0%. The increase in solids content is due to the reduction in the amount of aqueous culture medium incorporated in the harvested BNC membranes as longer incubation times are used. The previous is in line with the reduction in pellicle porosity observed in Figure 4 (SEM) for dried BNC membranes harvested after 5 and 21 days of fermentation. An increased microporosity has previously been proposed as a cause for larger volumes of water being collected in hydrophilic BNC membranes.^{15,29}

As shown, BNC obtained within 5 days [Figure 4 (a–b)] is composed of a highly reticulated 3D microfibril network. Ribbon-shaped cellulose nanofibers and nanofiber aggregates, with widths in the range of 18 to 57 nm (average value obtained from 150 measurements = 32.3 nm, SD = 6.7 nm) and micrometers in length, can be clearly distinguished. The presence of microfibril aggregates is due to the high density of hydroxyl groups on the surface of the microfibrils, which can strongly interact and lead to agglomeration.³⁰ The width dimensions are

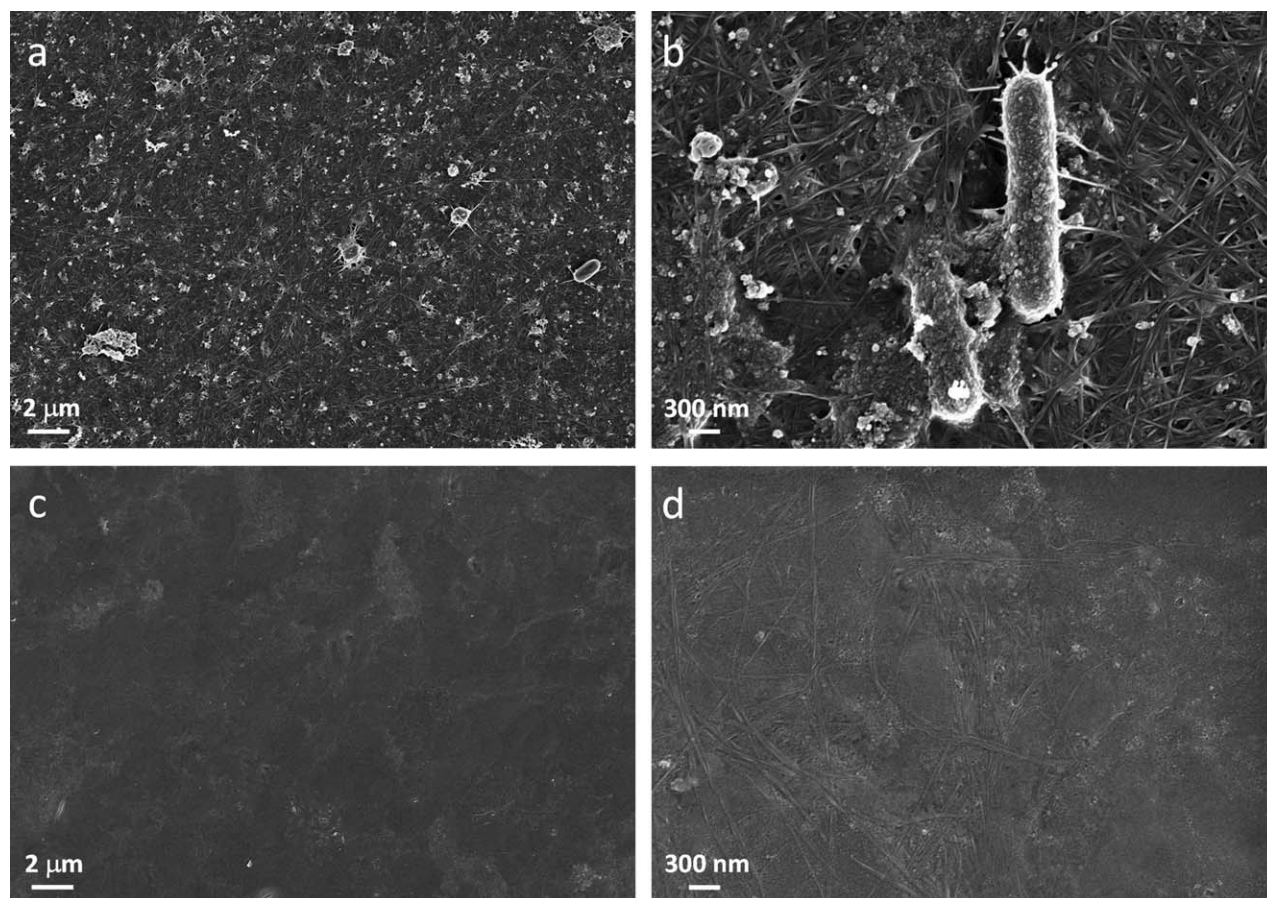


Figure 4. Bacterial nanocellulose from grape pomace obtained after 5 (a–b) and 21 days (c–d) of fermentation.

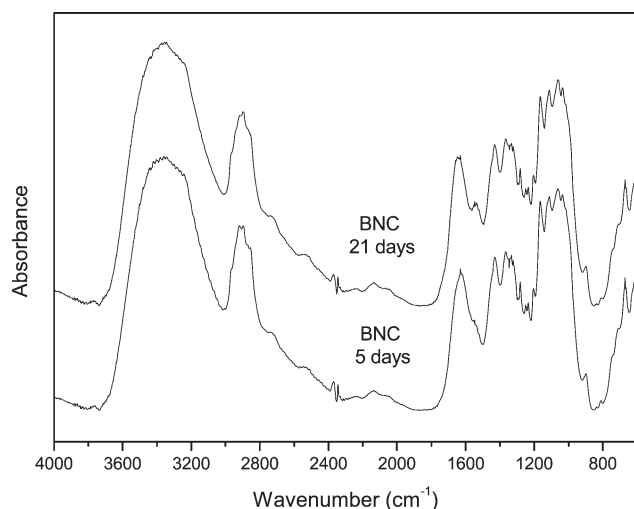


Figure 5. FTIR spectra of BNC pellicles obtained after 5 and 21 days of fermentation.

similar to those reported in the literature.^{31,32} Within the reticulated BNC structure, some trapped producing bacteria [(Figure 4(b)] and insoluble residues (i.e., corn steep liquor, grape bagasse) from the culture medium can still be seen.

Pellicles obtained after 21 days looked much more compact than the ones obtained after 5 days. Accordingly, scanning electron micrographs of the dried 21-day membrane [Figure 4(c–d)] confirmed a much more densely coagulated microfibril network, in which nanofibers seem to have been compressed, and their individual limits cannot be clearly distinguished. Sheykh-nazari *et al.*³³ reported that increasing the incubation time of *G. xylinus* up to 14 days in glucose- or mannitol-containing media improved the number of microfibril branches crossing each other, the number of bundles formed, and the H and C–H bonds generated. In terms of nanofiber dimensions, the denser 21-day BNC pellicle shows nanofibers that are micrometers in length and nanofiber bundles with widths in the range of 15 to 47 nm (average value obtained from 110 measurements: 29.1 nm, SD = 6.2 nm). The differences between the widths measured in both pellicles are not significant considering the difficulty of the measurement, especially in the highly compressed 21-day pellicle.

The FTIR spectra of dried BNC pellicles obtained within 5 and 21 fermentation days are shown in Figure 5. The bands observed in both spectra are those typical of bacterial nanocellulose: 3360 cm^{-1} (stretching vibration of hydroxyl groups), 2895 cm^{-1} (C–H stretching), 1630 cm^{-1} (absorbed water molecules), 1430 cm^{-1} (C–O bond stretching and CH_2 bending), 1368 cm^{-1} (C–H bending), 1333 cm^{-1} (O–H in-plane bending), 1321 cm^{-1} (CH_2 wagging), 1281 cm^{-1} (C–H bending), 1232 cm^{-1} (O–H in-plane vibration), 1170–1060 cm^{-1} (C–O–C groups of glycosidic bonds), and 898 cm^{-1} (β -linked glucose polymers).^{9,13,14,17} Moreover, it is well known that BNC is a composite of the two crystalline phases cellulose $I\alpha$ and $I\beta$ ($I\alpha/I\beta = 65/35$).^{34,35} The difference between the allomorphs consists in the H-bonding systems and in the conformation of neighboring cellulose chains.³⁶ The presence in both BNC pel-

licles of the triclinic $I\alpha$ allomorph and the monoclinic $I\beta$ allomorph of cellulose is confirmed by the shoulders observed in Figure 5 at 3241 cm^{-1} and 750 cm^{-1} and the shoulder shown at 710 cm^{-1} , respectively.^{9,37–39}

A comparison between the spectra indicated that the only difference between them was the intensity of the absorbance found at 1540 cm^{-1} , which corresponds to the bending vibration of N–H bonds.⁴⁰ The existence of nitrogenated compounds in BNC pellicles can be attributed to nutrient medium residues remaining in the samples. This is in line with SEM images that showed culture medium residues. The mentioned band is more intense in the spectrum of the 21-day pellicle, which may be explained in terms of its denser intertwined nanofibril structure (as evidenced from Figures 2 and 3), which makes the removal of trapped residues and remaining bacteria more difficult. The presence of nitrogenated nutrient medium residues (e.g., ammonia ions) in 1% NaOH autoclaved/water-washed BNC samples has been reported before.³¹

Cellulose is known to have different polymorphs (I, II, III, and IV), which have all been a matter of much study. Cellulose I is the crystalline cellulose that is naturally produced by trees, plants, algae, tunicates, and bacteria. Of the two different polymorphs of cellulose I, with a triclinic structure ($I\alpha$) and a monoclinic structure ($I\beta$), the $I\alpha$ structure is the dominant polymorph in bacterial nanocellulose.^{4,41} The $I\alpha$ unit cell parameters, space group P1, are $a = 0.672$ nm, $b = 0.596$ nm, $c = 1.040$ nm, $\alpha = 118.08^\circ$, $\beta = 114.80^\circ$, $\gamma = 80.375^\circ$.⁴² The diffraction patterns obtained for dried BNC pellicles collected within 5 and 21 fermentation days and peak assignments⁴³ are shown in Figure 6. The data gathered for the pellicle obtained after 30 days of incubation have also been included in order to study the evolution pattern with fermentation time.

The XRD patterns of BNC membranes obtained at increasing incubation times show a kinetics of phase formation. Moreover, an increase of crystalline material is registered for longer fermentation times. The gradual formation of the crystalline planes

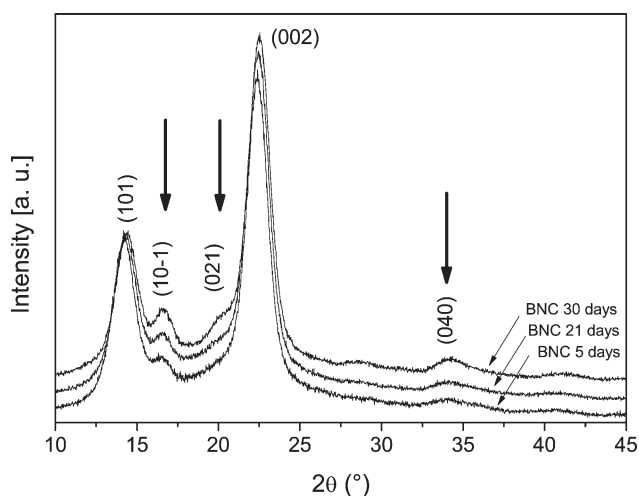


Figure 6. XRD patterns of dried BNC samples harvested after 5, 21, and 30 days and the corresponding Miller indices. The gradual formation of peaks of less intensity is indicated by arrows.

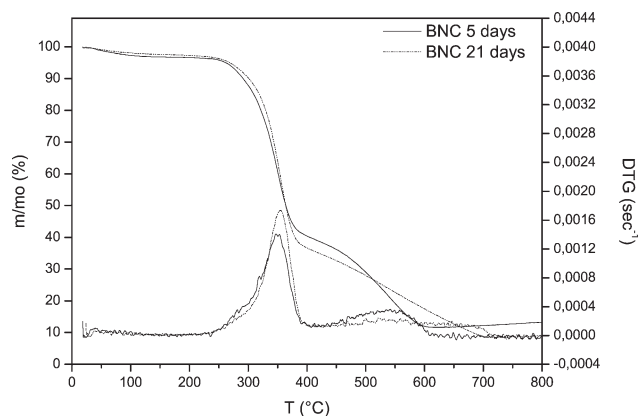


Figure 7. TG and DTG curves of BNC pellicles obtained after 5 and 21 days of fermentation.

associated with the peaks of less intensity, i.e., (10-1), (021), and (040), are evidence of such an increase.

A Lorentz function was used to fit the XRD peak profiles in order to determine their relative area in the XRD pattern. From the ratio between the XRD peak area and the XRD pattern area, the crystallinity (C) of the BNC samples was estimated. The increase in the fermentation time caused an increase in the sample crystallinity for the longest times. The estimated value of C is 68% for the 5-day BNC pellicle, 68% for the 21-day pellicle, and 85% for the BNC obtained after 30 days. The change of the XRD peak intensity ratio and the increase of the sample's crystallinity are evidence of a reordering of the BNC crystal structure as a function of the fermentation time.

In order to know if the structural reordering increases the crystallite size (D), the average value of D was estimated from the Scherrer equation.⁴⁴ The estimated D value (5.5, 5.2, and 5.3 nm for 5, 21, and 30 days of fermentation, respectively) was around 5 nm for all BNC samples, meaning that D is not dependent on fermentation time.

Figure 7 collects the TG and DTG curves of dried BNC membranes harvested after 5 and 21 days of fermentation. The DTG data have been normalized with respect to the initial sample mass. For both membranes, the TG data showed three weight-loss steps. The first weight loss occurred from room temperature to 130 °C, and it is assigned to BNC dehydration. In this step, membrane moisture that could not be removed during preconditioning (110 °C, 1 h) was evaporated. For both pellicles, the removed moisture content during this step accounted for 3–4% (three replicates).

The second weight loss observed in Figure 7 is assigned to cellulose decomposition.⁴⁵ For the 5-day pellicle, the second weight loss was characterized by T_{onset} and T_{max} temperatures of 304.5 ± 0.5 °C and 349 ± 3 °C, respectively. For the 21-day membrane, T_{onset} and T_{max} were found at 314 ± 3 °C and 350 ± 4 °C, respectively. The calculated T_{onset} and T_{max} values of the second weight loss suggest that whereas the maximum weight-loss rate temperature T_{max} is not affected by the age of the pellicles, the beginning of their decomposition does vary (results based on three replicates). The higher-onset decomposi-

tion temperature found for the 21-day pellicle could be attributed to the increased number of effective hydrogen bonds between BNC nanofibers, which are more closely packed than the microfibrils forming the 5-day membrane. Differences in onset decomposition temperatures of neat and modified bacterial nanocellulose have previously been correlated with microfibril packing efficiency.²²

Extending the TG analysis up to 800 °C evidenced the presence of a third smaller weight loss, between 450 and 600 °C. This high-temperature weight loss has previously been attributed to the degradation of polymeric chains and the six-member cyclic structure, pyran, distinguishing it from the previous decomposition step assigned to the removal of molecular fragments such as hydroxyl and hydroxymethyl groups.²⁹ The TG and DTG data also showed a difference between the 5-day and 21-day BNC membranes for this third weight loss, evidencing a slightly sharper mass decrease in the case of the 5-day pellicle. The sharper decrease of the TG curve of the 5-day pellicle could be due to a probably lower molecular weight that is due to lower incubation time.

A DMA analysis was performed on dried BNC pellicles obtained after 5 and 21 days of fermentation in tension mode. The assay gave information on the initial storage modulus (E_0) of the membranes, which accounted for 2.9 ± 0.3 GPa for the 5-day pellicle and 4.9 ± 0.9 GPa for the 21-day pellicle ($T = 32$ °C). The initial storage modulus of the 30-day pellicle was also measured to confirm the pattern, giving a value of 5.8 ± 0.4 GPa. The results obtained show that as more days are given to the BNC synthesis, the dried membranes display a higher initial storage modulus, which is explained in terms of the denser network structure of the older pellicles in which more fiber–fiber interactions through hydrogen bonding are possible. In the case of the oldest pellicle, its higher crystallinity should also be considered. Lower interfibrillar space in compressed BNC membranes has previously been reported by Retegi *et al.*³² as the cause of important increases in elastic modulus values, attributed to a higher contribution of interfibrillar bonding zones. In fact, these authors observed that the elastic modulus of compressed BNC pellicles increased with a nearly linear dependence on the increase of cellulose volume fraction in the films. In the acetylation of BNC pellicles, Hu *et al.*⁴⁶ observed that the Young's modulus of acetylated BNC was lower than that of neat BNC, and they attributed the difference to the lower degree of crystallinity and the less-dense network structure obtained upon the introduction of acetyl groups.

In reference to the effect of temperature on the storage modulus values, within the assayed temperature interval (30–100 °C) the values showed a slight increase with temperature (in all cases lower than 6%), which is explained in terms of additional dehydration of the pellicles during the analysis (data not shown). According to the literature, no transitions were expected to be found within the range of temperature scanned.

CONCLUSIONS

BNC production by *G. xylinus* using an abundant waste of the wine industry and a byproduct of corn starch production was

statistically optimized. The grape pomace/corn steep liquor medium proposed resulted in a high production of BNC, actually more than four times higher than that achieved in the Hestrin and Schramm medium in identical conditions.

Characterization of dried BNC harvested at different incubation times evidenced that older pellicles have a more densely coagulated microfibril network. The higher probability of interfibrillar interactions through hydrogen bonding in BNC pellicles obtained after longer incubation times is proposed to be the cause for their higher-onset decomposition temperature and higher initial storage modulus measured. An increase of crystalline material was also registered for the highest fermentation time.

The results obtained in the current contribution demonstrate that high BNC production can be achieved in an inexpensive medium formulated with grape bagasse and corn steep liquor as major C and N sources. Moreover, the usefulness of experimental design and optimization methodologies for maximizing the response with a much lower number of assays than classic approaches has been demonstrated. Finally, the important impact of incubation time on nanofiber density, and as a consequence on thermal stability, crystallinity, and storage modulus of the dried BNC pellicles obtained, has also been illustrated. Although, considering mainly production issues, BNC pellicles obtained in a static culture are generally harvested at long fermentation times, the results shown herein have demonstrated that incubation time should be considered as a useful variable for tailoring the properties of BNC pellicles.

ACKNOWLEDGMENTS

The authors acknowledge Dr. Luis Ielpi (Fundación Instituto Leloir, Buenos Aires, Argentina) for the bacterial strain; Dr. Mariana Combina (Estación Experimental Agropecuaria, Instituto Nacional de Tecnología Agropecuaria, Mendoza, Argentina) and Dr. Cecilia Rojo (Estación Experimental Agropecuaria, Instituto Nacional de Tecnología Agropecuaria, Mendoza, and CONICET, Argentina) for grape pomace; Ingredion Argentina S.A. for corn steep liquor; Dr. Juan Pablo Morales Arias and Dr. María José Batiller for technical training in DMA analysis; and Agencia Nacional de Promoción Científica y Tecnológica (PICT 00223 2008 – PRE-STAMO BID), Consejo Nacional de Investigaciones Científicas y Técnicas (CONICET – PIP 11220110100608), and Universidad de Buenos Aires (UBACYT 20020090100065) for financial support.

REFERENCES

1. Chawla, P. R.; Bajaj, I. B.; Shrikant, A. S.; Singhal, R. S. *Food Technol. Biotech.* **2009**, *47*, 107.
2. De Souza Lima, M. M.; Borsali, R. *Macromol. Rapid Commun.* **2004**, *25*, 771.
3. Horikawa, Y.; Sugiyama, J. *Biomacromolecules* **2009**, *10*, 2235.
4. Moon, R. J.; Martini, A.; Nairn, J.; Simonsen, J.; Youngblood, J. *Chem. Soc. Rev.* **2011**, *40*, 3941.
5. Sani, A.; Dahman, Y. *J. Chem. Technol. Biotechnol.* **2010**, *85*, 151.
6. Dahman, Y.; Jayasuriya, K. E.; Kalis, M. *Applied Biochem. Biotechnol.* **2010**, *162*, 1647.
7. Wu, J.; Liu, R. J. *Biosci. Bioeng.* **2013**, *115*, 284.
8. Carreira, P.; Mendes, J. A. S.; Trovatti, E.; Serafim, L. S.; Freire, C. S. R.; Silvestre, A. J. D.; Neto, C. P. *Biores. Technol.* **2011**, *102*, 7354.
9. Castro, C.; Zuluaga, R.; Putaux, J. L.; Caroa, G.; Mondragon, I.; Gañan, P. *Carbohydr. Polym.* **2011**, *84*, 96.
10. Goelzer, F. D. E.; Faria-Tischer, P. C. S.; Vitorino, J. C.; Sierakowski, M. R.; Tischer, C. A. *Mater. Sci. Eng. C* **2009**, *29*, 546.
11. Hong, F.; Qiu, K. *Carbohydr. Polym.* **2008**, *72*, 545.
12. Moosavi-Nasab, M.; Yousefi, M. *Iran. J. Biotechnol.* **2011**, *9* (2), 94.
13. Rani, M. U.; Navin, K. R.; Anu Appaiah, K. A. J. *Microbiol. Biotechnol.* **2011**, *21*, 739.
14. Vazquez, A.; Foresti, M. L.; Cerrutti, P.; Galvagno, M. J. *Polym. Environ.* **2013**, *21*, 545.
15. Algar, I.; Fernandes, S. C. M.; Mondragon, G.; Castro, C.; Garcia-Astrain, C.; Gabilondo, N.; Retegi, A.; Eceiza, A. J. *Appl. Polym. Sci.* **2015**, *132*, 41237.
16. Santos, S. M.; Carbajo, J. M.; Villar, J. C. *Biores.* **2013**, *8*, 3630.
17. Mateo, J. J.; Maicas, S. *Food Res. Int.* **2015**, *73*, 13.
18. Strobel, R. J.; Sullivan, G. R. In *Manual of Industrial Microbiology and Biotechnology*; Demain, A.; Davies, J., Eds.; ASM Press: Washington DC, **1999**; Chapter 6, pp 80–93.
19. Montgomery, D. C. In *Designs and Analysis of Experiments*; John Wiley & Sons: New York, **2001**; Chapter 6.
20. Box, G. E. P.; Behnken, D. W. *Technomet.* **1960**, *2*, 455.
21. Ilharco, L. M.; Gracia, R. R.; da Silva, J. L.; Ferreira, L. F. V. *Langmuir* **1997**, *13*, 4126.
22. Lee, K. Y.; Quero, F.; Blaker, J. J.; Hill, C. A. S.; Eichhorn, S. J.; Bismarck, A. *Cellulose* **2011**, *18*, 595.
23. Al-Abdallah, W.; Dahman, Y. *Bioproc. Biosyst. Eng.* **2013**, *36*, 1735.
24. Carreño Pineda, L. D.; Caicedo Mesa, L. A.; Martínez Riascos, C. A. *Ing. Cienc.- Universidad EAFIT* **2012**, *8*, 307.
25. Zeng, X.; Small, D. P.; Wan, W. *Carbohydr. Polym.* **2011**, *85*, 506.
26. Wang, Z. G.; Wei, Y. L.; Wei, M. S.; Wang, X. B.; Xiang, D. *Food Sci.* **2008**, *29*, 295.
27. Matsuoka, M.; Tsuchida, T.; Matsushita, K.; Adachi, O.; Yoshinaga, F. *Biosci. Biotechnol. Biochem.* **1996**, *60*, 575.
28. Klemm, D.; Kramer, F.; Moritz, S.; Lindström, T.; Ankerfors, M. D.; Dorris, A. *Angew. Chem. Int.* **2011**, *50*, 5438.
29. Cheng, K.-C.; Catchmark, J. M.; Demirci, A. *Cellulose* **2009**, *16*, 1033.
30. Zimmermann, T.; Pohler, E.; Geiger, T. *Adv. Eng. Mater.* **2004**, *6*, 754.
31. Ciechańska, D.; Wietecha, J.; Kaźmierczak, D.; Kazimierczak, J. *Fibres Text. East. Eur.* **2010**, *18*, 98.

32. Retegi, A.; Gabilondo, N.; Peña, C.; Zuluaga, R.; Castro, C.; Gañán, P.; de La Caba, K.; Mondragon, I. *Cellulose* **2010**, *17*, 661.
33. Sheykhnazari, S.; Tabarsa, T.; Ashori, A.; Shakeri, A.; Golalipour, M. *Carbohydr. Polym.* **2011**, *86*, 1187.
34. Atalla, R. H.; Vanderhart, D. L. *Science* **1984**, *223*, 283.
35. Yamamoto, H.; Horii, F.; Hirai, A. *Cellulose*, **1996**, *3*, 229.
36. Klemm, D.; Schumann, D.; Kramer, F.; Heßler, N.; Hornung, M.; Schmauder, H. P.; Marsch, S. *Adv. Polym. Sci.* **2006**, *205*, 49.
37. Kataoka, Y.; Kondo, T. *Macromolecules* **1996**, *29*, 6356.
38. Kose, R.; Mitani, I.; Kasai, W.; Kondo, T. *Biomacromolecules* **2011**, *12*, 716.
39. Sugiyama, J.; Persson, J.; Chanzy, H. *Macromolecules* **1991**, *24*, 2461.
40. Coates, J. P. In *Encyclopedia of Analytical Chemistry*; Meyers, R. A., Ed.; John Wiley & Sons: Chichester, UK, **2000**; A Practical Approach to the Interpretation of Infrared Spectra, p 10815.
41. Yamamoto, H.; Horii, F. *Cellulose* **1994**, *1*, 57.
42. Nishiyama, Y.; Sugiyama, J.; Chanzy, H.; Langan, P. J. *Am. Chem. Soc.* **2003**, *125*, 14300.
43. Park, S.; Baker, J. O.; Himmel, M. E.; Parilla, P. A.; Johnson, D. K. *Biotechnol. Biofuels* **2010**, *3*, 1.
44. Klug, H.; Alexander, L. In *X-ray Diffraction Procedures for Polycrystalline and Amorphous Materials*, 2nd ed.; New York: John Wiley and Sons: **1974**.
45. Barud, H. S.; Ribeiro, C. A.; Capela, J. M. V.; Ribeiro, S. J. L.; Messadeq, Y. J. *Therm. Anal. Calorim.* **2011**, *105*, 421.
46. Hu, W.; Chen, S.; Xu, Q.; Wang, H. *Carbohydr. Polym.* **2011**, *83*, 1575.
47. Kennedy, M.; Krouse, D. J. *Ind. Microbiol. Biotechnol.* **1999**, *23*, 456.
48. Box, G. E. P.; Hunter, W.; Hunter, J. In *Estadística para Investigadores*; Reverté, Ed.; John Wiley & Sons: Barcelona, **1999**; Chapter 3, p 109.